



# Cytotoxicity Effect and Antibacterial Activity of $\text{Al}_2\text{O}_3$ Nanoparticles Activity against *Streptococcus Pyogenes* and *Proteus Vulgaris*

<sup>1</sup>Anwar Sabri Jawad, <sup>1</sup>Qasim Najem Obaid Thewaini, <sup>2</sup>Sharafaldin Al-Musawi\*

<sup>1</sup>College of Biotechnology, Al-Qasim Green University, Babylon Province, Iraq

<sup>2</sup>College of Food Sciences, Al-Qasim Green University, Babylon Province, Iraq

## Article information

### Article history:

Received: June, 28, 2021

Accepted: July, 27, 2021

Available online: September, 18, 2021

### Keywords:

Antibacterial,  
Cytotoxicity,  
Aluminum oxide nanoparticles

### \*Corresponding Author:

Qasim Najem Obaid Thewaini  
[thewaini@biotech.uoqasim.edu.iq](mailto:thewaini@biotech.uoqasim.edu.iq)

## Abstract

Aluminum oxide, often known as  $\text{Al}_2\text{O}_3$ , is a chemical compound of aluminum and oxygen with the formula  $\text{Al}_2\text{O}_3$ . It's the most common of many aluminum oxides, known as aluminum (III) oxide. The study investigates the cytotoxicity and antibacterial effects of Aluminum oxide nanoparticles ( $\text{Al}_2\text{O}_3$ -NPs) in different cells and bacteria. Different characterization methods such as dynamic light scattering (DLS), field emission scanning electron microscopy (FESEM), X-ray diffraction (XRD), and Fourier transform infrared spectroscopy (FTIR) have been used to evaluate morphologies and physicochemical properties of  $\text{Al}_2\text{O}_3$ -NPs. MTT technique is used for determining NPs cytotoxicity. The size distribution of  $\text{Al}_2\text{O}_3$ -NPs was  $68 \pm 12$  nm in diameter, while the zeta potential was  $(-36 \pm 10$  mV). There is no toxicity by using the MTT assay, as well as showed antibacterial activity was formed at 200  $\mu\text{g/mL}$ , while the higher antibacterial activity was occurring at  $(18 \pm 0.2)$  and  $(17 \pm 0.1)$  for *Proteus Vulgaris* and *Streptococcus pyogenes*, respectively. The findings confirmed that the  $\text{Al}_2\text{O}_3$ -NPs have small dimensions, high stability, and increased antibacterial activity.

DOI: [10.53293/jasn.2021.3944.1061](https://doi.org/10.53293/jasn.2021.3944.1061), Department of Applied Science, University of Technology

This is an open access article under the CC BY 4.0 License

## 1. Introduction

$\text{Al}_2\text{O}_3$ -NPs are white, odorless crystalline powder. These NPs are water-insoluble in both physical and chemical conditions, and their dimensions vary according to the method of preparation. Different crystalline modifications are generated and utilized broadly in a wide range of products medicinal, domestic, and manufactured products. The prevalence of microbial infections poses a significant threat to global public health. Antibiotics are a standard treatment for treating bacterial infections due to their cost-efficacy and positive effect. However, numerous studies have shown clearly that extensive antibiotic use has contributed to the development of multidrug-resistant bacterial strains [1,2]. More recently, metallic nanomaterials have become highly attractive and rapidly emerging materials in different scientific fields [3-7]. The significant interest of nanomaterial research and development, particularly NPs, is due to their attractive characteristics, revealed by their small size, unusual high surface area activity offering excellent catalytic, optical, and electrical properties [8-10]. Therefore, Metallic NPs have been active in comprehensive research, methods, and advanced micro-and nanotechnology

applications [1,11-16]. Due to their unique physicochemical properties in biological applications, metal oxide NPs like iron oxide NPs ( $\text{Fe}_3\text{O}_4$ ), manganese oxide NPs ( $\text{MgO}$ ), titanium dioxide NPs ( $\text{TiO}_2$ ), zinc oxide NPs ( $\text{ZnO}$ ). These NPs used widely during the last years.  $\text{Al}_2\text{O}_3$ -NPs are a metallic NPs that has been used as an antimicrobial agent in the previous ten years. This NPs is used in medicine due to it has minimal toxicity [17].  $\text{Al}_2\text{O}_3$ -NPs have good antimicrobial activity against a broad spectrum of pathogenic bacteria, even in low doses. Simultaneously, they may be caused complete growth inhibition of bacteria at only a few  $\mu\text{g/ml}$  concentrations. These NPs have been proven valuable agents for inhibiting antibiotic-resistant bacteria and developing resistance strains [18]. In this work, the in vitro study of  $\text{Al}_2\text{O}_3$ -NPs was performed by antibacterial activity and cytotoxicity effect to determine the effectiveness of these NPs on some specific colonies of *S. pyogenes* and *P. Vulgaris*. Characterization of  $\text{Al}_2\text{O}_3$ -NPs was studied using FESEM, FTIR, DLS, and XRD.

## 2. Materials and methods

$\text{Al}_2\text{O}_3$ -NPs (Mw of 136.29) were purchased from skyspring Nanomaterials, Inc, USA. Muller Hinton media was providing by Himedia, India. Aquacel®Ag is provided by ConvaTec Company, England. Dulbecco's Modified Eagle Medium (DMEM), MTT (3-(4,5-dimethylthiazol-2-yl)-2,5-diphenyltetrazolium bromide) powder, Phosphate-Buffered Saline (PBS), Fetal Bovine Serum (FBS) were purchased from Sigma Aldrich (Sydney, Australia).

### 2.1. Characterization of $\text{Al}_2\text{O}_3$ -NPs

The shape, size, and morphological properties of  $\text{Al}_2\text{O}_3$ -NPs characterized using FESEM (Hitachi S-4800 II, Japan) with 20kV and the TEM (Hitachi H-7650, Tokyo, Japan) at an acceleration voltage of 80 kV. The hydrodynamic size and zeta potential of the  $\text{Al}_2\text{O}_3$ -NPs were measured using DLS (Horiba SZ-100 nanoparticle analyzer). For XRD analysis, the  $\text{CuK}\alpha$  ( $\lambda = 1.54056 \text{ \AA}$ ) in Bragg-Brentano were produced using a Phillips X'pert 1710 diffractometer. The voltage used was 40 kV, and the current intensity was 25 mA. The FTIR analysis was performed in Shimadzu Corporation, Japan. For this purpose, the prepared samples were analyzed over a wavelength range of 400–4000  $\text{cm}^{-1}$  to determine the specimens 'functional groups.

### 2.2. MTT assay

To measure the cytotoxic effect and biocompatibility of prepared  $\text{Al}_2\text{O}_3$ -NPs, (MTT) assay was used following instruction from the manufacturer. Vero cell culture was incubated at  $37^\circ\text{C}$  in 5%  $\text{CO}_2$ . The extracted solutions are filtered by filters (0.22  $\mu\text{m}$ , sigma company, united states American). Preparation of the DMEM is performed at several dilutions (50, 100, 150, and 200 $\mu\text{g/ml}$ ) of the extract. The Vero cells (ATCC® CCL-81™) ( $1 \times 10^4$  cells/well) were kept for one day in 96 wells at  $37^\circ\text{C}$ . Afterward, the cells were treated with the extract solutions with several dilution ratios for two days. Then, add the MTT solution (20  $\mu\text{l}$ ) to all the wells and hold for 4 hours. DMSO (100  $\mu\text{l}$ ) was added for the dissolving of the formazan. At the wavelength of 590, the O.D. was determined for each sample [18].

### 2.3. Antibacterial activity

Kirby-Bauer used the disk diffusion method to test antibacterial activity [19] was considered a suitable method for evaluating the antibacterial activity of  $\text{Al}_2\text{O}_3$ -NPs. A sterile inoculating loop was briefly collected from four or five bacterial colonies and suspended in 2ml of sterilized PBS. The studied bacteria, including *S. Pyogenes* and *P. Vulgaris*. The bacteria suspension turbidity has been modified to 0.5 McFarland level by diluting with sterile PBS. Sterile swabs have been inserted into the inoculum channels. Muller–Hinton agar plates inoculated with bacteria by streaking swabs. Dissolve 0.1 mg  $\text{Al}_2\text{O}_3$ -NPs powder in 1ml of distilled water to disperse  $\text{Al}_2\text{O}_3$ -NPs suspension. The suspension has been sonicated 10 min before use. A 40  $\mu\text{l}$  of  $\text{Al}_2\text{O}_3$ -NPs suspension, distilled water (as negative control), and HCl (as positive control) have been impregnated into the standard antibiotic disk. Lastly, all disks were used to evaluate antibacterial activity in Mueller-Hinton (Merck, Germany) against two types of bacterial strains. Impregnated disks were placed with sterile forceps on the surface of the agar. Plates were incubated for 24 h at  $37^\circ\text{C}$  to control antibacterial activity; the activity (inhibition zone) was measured by millimeters, the tests were done three times.

### 2.4. Statistical analysis

The mean  $\pm$  standard division (S.D.) was used for the statistical analysis of our results. Excel was also used to evaluate statistical significance. Results  $p < 0.05$  and  $p < 0.01$  are defined as the criteria for statistical significance.

### 3. Results and Discussion3.1 Characterization of $\text{Al}_2\text{O}_3$ -NPs

To evaluate the size and morphology characteristics of the  $\text{Al}_2\text{O}_3$ -NPs, FESEM and HRTEM were performed. Both FESEM and HRTEM images presented that synthesized  $\text{Al}_2\text{O}_3$ -NPs have a spherical shape with a nanoscale size and notable dispersion ratio (Figure 1). For the XRD (figure 2) test, the Cu – Ka-wavelength ( $T_\lambda = 1.5405 \text{ \AA}$ ) was used via a Phillips diffractometer using powder samples of  $\text{Al}_2\text{O}_3$ -NPs. The voltage used was 35 kV, and the current intensity was 30 mA.

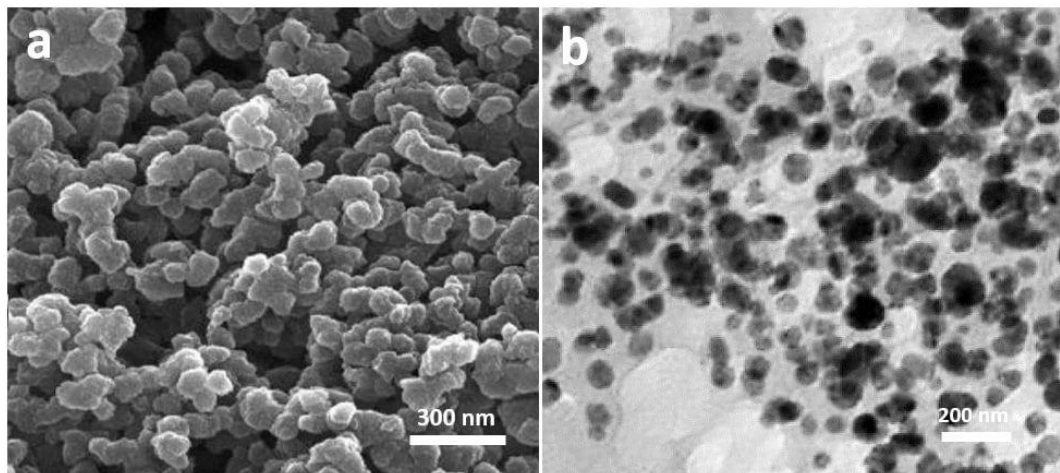


**Figure 1:** SEM (a) and TEM (b) images of synthesized gamma-alumina.

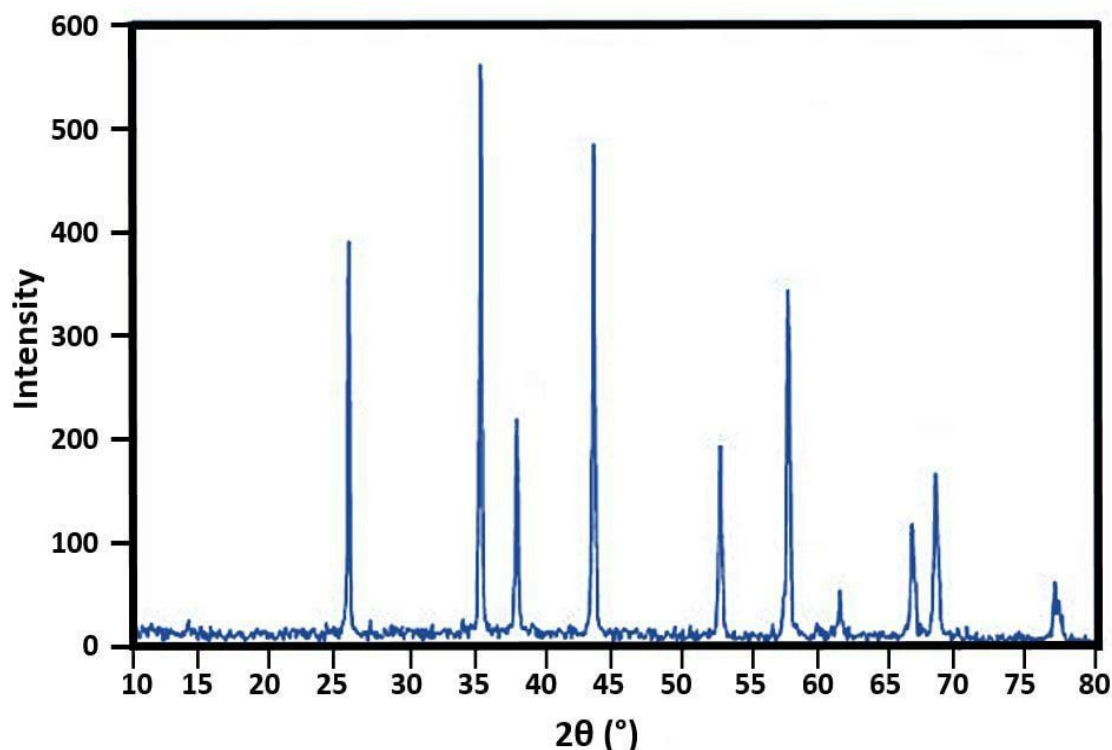


**Figure 2:** XRD pattern of synthesized gamma-alumina.

The DLS analysis was done to study the hydrodynamic diameter and charge of  $\text{Al}_2\text{O}_3$ -NPs (Figure 3). DLS showed small bodies with a hydrodynamic  $\text{Al}_2\text{O}_3$ -NPs of  $68 \pm 12 \text{ nm}$  and  $-36 \pm 10 \text{ mV}$  in diameter and charge, respectively. The study on prepared suspension also confirms the general zeta potential criteria negatively for improved stability. Previous studies confirmed that the zeta assay was used to determine the cell interactions,

cell diagnosis, and normal and cancer-cell effect therapeutics had been measured [20-22]. In the FTIR experiment, the Al-OH vibrations were in the vibrational frequencies of 1551 and 1615  $\text{cm}^{-1}$ . This analysis also found that the absorption in the frequencies of 642  $\text{cm}^{-1}$  and 970  $\text{cm}^{-1}$  increased, which is related to the sites of octahedral AlO<sub>6</sub> and tetrahedral AlO<sub>4</sub>, suggesting the phase change into the state  $\alpha$ -alumina in the 4% dopant [20].

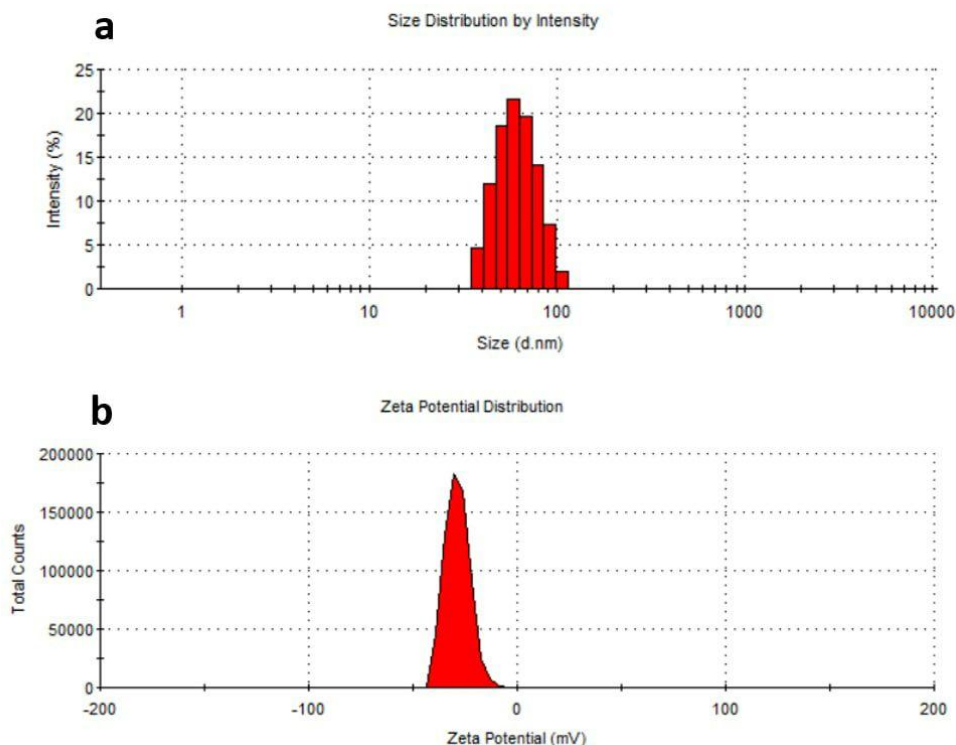


**Figure 3:** Size distribution and zeta potential of Al<sub>2</sub>O<sub>3</sub>-NPs.

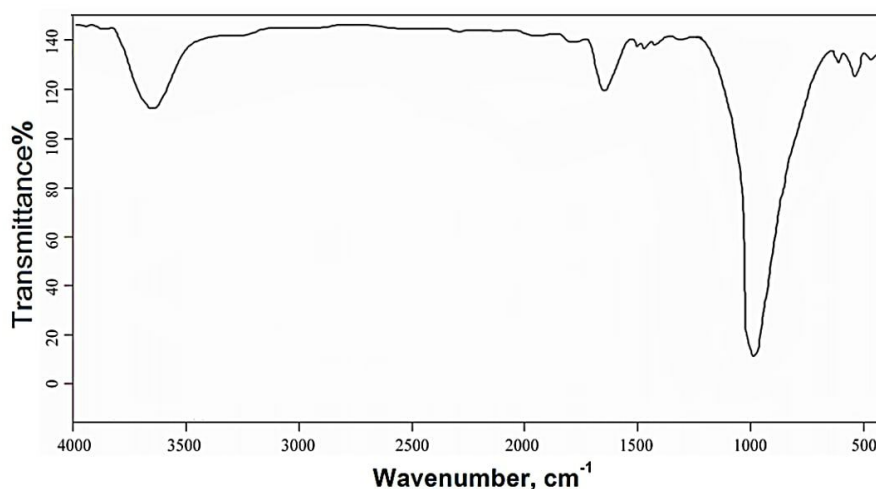


**Figure 4:** FTIR analysis was used to determine the functional groups of Al<sub>2</sub>O<sub>3</sub>-NPs.

### 3.1. MTT results

The MTT assay was used to evaluate the viability/proliferation of Al<sub>2</sub>O<sub>3</sub>-NPs at various concentrations, 50 mg/ml, 100 mg/ml, 150 mg/ml, and 200 mg/ml on Vero cell lines for 24 h (Figure5). Compared to the control group (without Al<sub>2</sub>O<sub>3</sub>-NPs), the samples' did not show any cytotoxicity at mentioned concentrations for 24 h.

$\text{Al}_2\text{O}_3$ -NPs is induced endothelial leakiness and improves nanomedicine's biodistribution to target sites [23-25]. Several studies show that when the endothelial cells were exposed to  $\text{Al}_2\text{O}_3$ -NPs, it will cause leakiness of the endothelial cells and interfere with endothelial cells' adherens  $\text{Al}_2\text{O}_3$ -NPs and vascular endothelial cadherin. The leakiness of the endothelial cells is attributed to the toxic effects of inorganic NPs in the cells [26-28].

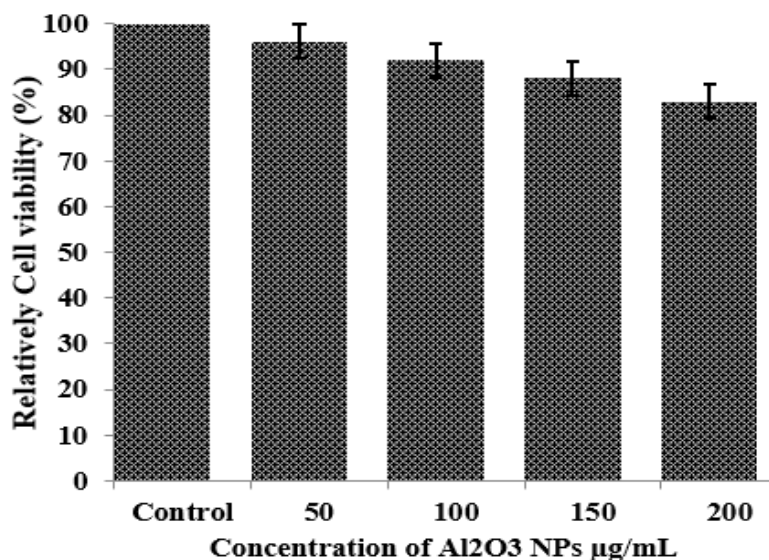


**Figure 5:** Showed the Vero cell lines treated with several doses of  $\text{Al}_2\text{O}_3$ -NPs for one day. Mean  $\pm$  standard error was expressed for the data from three replications.

### 3.2. Antibacterial activity

The synthesized  $\text{Al}_2\text{O}_3$ -NPs were used for antibiotic susceptibility at five concentrations (25, 50, 100, 150, and 200  $\mu\text{g/mL}$ ), as shown in Figure 6. The figure exhibits the inhibition zone  $\text{Al}_2\text{O}_3$ -NPs against tested bacteria. Figure 7 shows an exemplary diffusion assay that  $\text{Al}_2\text{O}_3$ -NPs were more efficient as antibacterial agents on *S. pyogenes* and *P. Vulgaris*. It showed antibacterial activity was formed at 200  $\mu\text{g/mL}$ , while the higher antibacterial activity was occurring at  $(18 \pm 02)$  and  $(17 \pm 01)$  for *P. Vulgaris* and *S. pyogenes*, respectively. The reduction of antibacterial activity may be due to the calcination of  $\text{Al}_2\text{O}_3$ -NPs, which caused an increase in particle size.  $\text{Al}_2\text{O}_3$ -NPs exhibited an interesting antibacterial decrease due to the enhancement of the specific surface area. The nature of  $\text{Al}_2\text{O}_3$ -NPs can explain this phenomenon, and one of the main mechanisms of its action is the production of reactive oxygen species (ROS) on its surface during the photocatalysis process when it is exposed to light at a suitable wavelength, which leads to phospholipid peroxidation and, finally cell death [29-33]. This study was carried out to strengthen further the physical-chemical properties of  $\text{Al}_2\text{O}_3$ -NPs by antibacterial activity. With a specific surface area, the crystalline category of our  $\text{Al}_2\text{O}_3$ -NPs, assesses the negative zeta potential of  $-36 \pm 10$  mV, besides the  $68 \pm 12$  nm average diameter in size. Many studies have been made to understand biomaterials biocompatibility effect on cells for produce osteointegration during the recent decades, such as prevailing environment, like adhesion, cell viability, and proliferation. The physicochemical properties like shape, size, phase purity, surface area, surface topography, particle concentration, crystalline structure, and surface charging greatly increase cell viability. However, Shi et al. [34]. have reported the potential side effects and beneficial activity of the conventional  $\text{Al}_2\text{O}_3$ -NPs. A profuse and overdoses, form, size, composition, crystalline properties, added functional groups, solubility, and the manufacture of impurities of such a heterogeneous nature was applied on many cell lines like lung cells, mucosal cells, cardiovascular cells, nerve cells, skin cells, reproductive cells, and kidney cells to study the activity of the titanium.

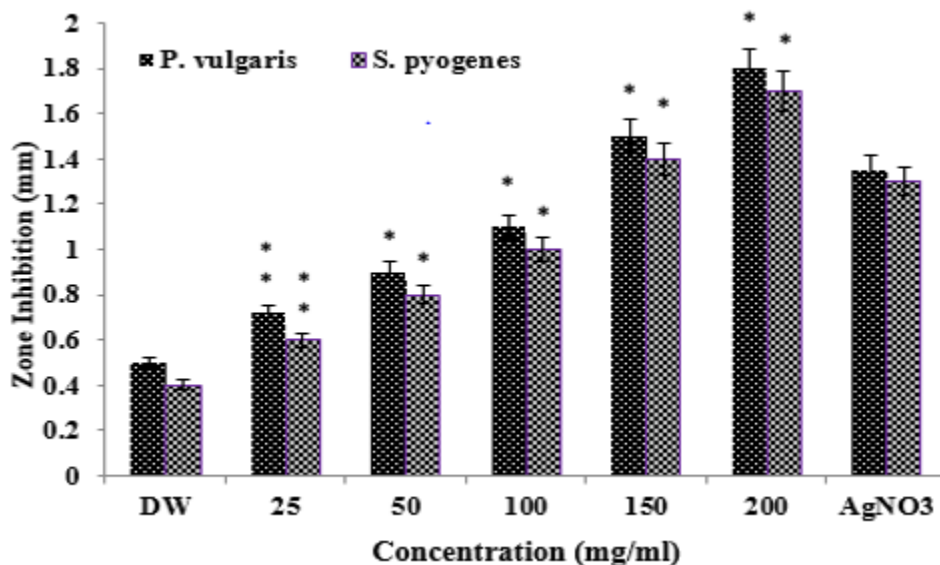


**Figure 6:** Antibacterial activity of  $\text{Al}_2\text{O}_3$ -NPs against *P.vulgaris* and *S.pyogenes*. mean  $\pm$  SD are presented for data for *p.vulgaris* and  $\text{AgNO}_3$  NPs at  $p < 0.01$  and  $p < 0.05$ .

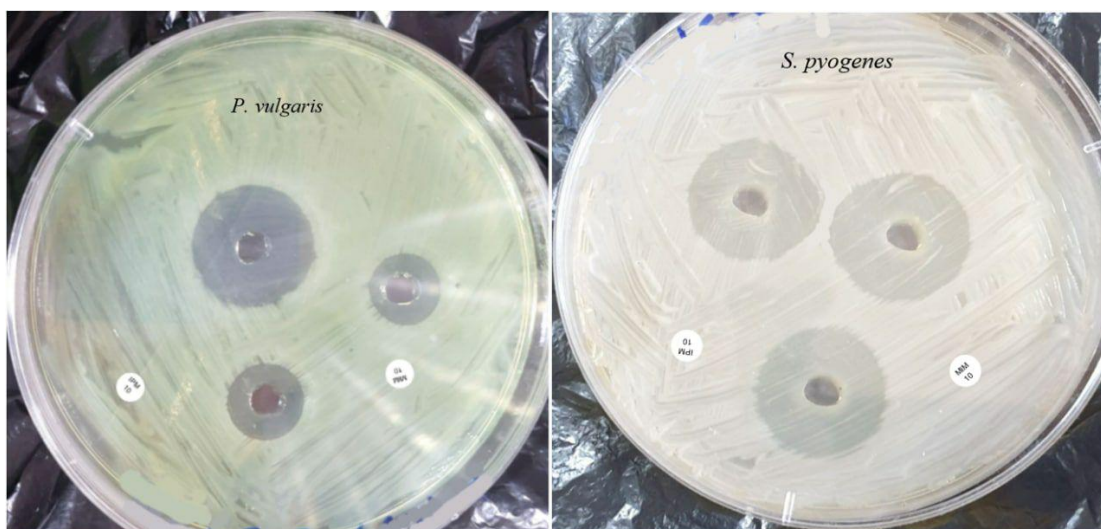


**Figure 7:** Well diffusion assay exhibiting the impact of  $\text{Al}_2\text{O}_3$ -NPs as antibacterial agents against *S.pyogenes* and *P.vulgaris*.

$\text{Al}_2\text{O}_3$ -NPs stuck in a suspension on bacterial surfaces and resulting in  $\text{Al}_2\text{O}_3$ -NPs being adsorbed on the surface of bacteria [35] that could lead in combination with a photocatalytic oxidation reaction to inactivating bacteria [36]. There are several possible mechanisms to explain bacteria's impact on  $\text{Al}_2\text{O}_3$ -NPs [37]. Not all antibiotics have synergistic antimicrobial effects when used with  $\text{Al}_2\text{O}_3$ -NPs since one study showed the lack of increased antibacterial activity using CEF antibiotics in combination with  $\text{Al}_2\text{O}_3$ -NPs. Compared to the CEF antibiotic combined with  $\text{Al}_2\text{O}_3$ -NPs, the CEZ antibiotic showed an excellent synergistic impact [38].

#### 4. Conclusions

This work studied the cytotoxicity and antibacterial effects of Aluminium  $\text{Al}_2\text{O}_3$ -NPs in different cells and bacteria. Different characterization methods such as DLS, FESEM, XRD, and FTIR, confirmed the morphologies and physicochemical properties of  $\text{Al}_2\text{O}_3$ -NPs. The size distribution and zeta potential of  $\text{Al}_2\text{O}_3$ -

NPs has been proved the suitability of this nanoparticle for antibacterial and cytotoxic studies. There is no toxicity by using the MTT assay, as well as showed antibacterial activity was formed at 200 µg/mL, while the higher antibacterial activity was occurring for *Proteus Vulgaris* and *Streptococcus pyogenes*, respectively. The findings confirmed that the Al<sub>2</sub>O<sub>3</sub>-NPs have small dimensions, high stability, and increased antibacterial activity.

#### Acknowledgment:

This work is supported by college of Biotechnology, Al-Qasim Green University, Babil, Iraq.

#### References

- [1] S. Albukhaty, L. Al-Bayati, H. Al-Karagoly, and S. Al-Musawi, "Preparation and characterization of titanium dioxide nanoparticles and in vitro investigation of their cytotoxicity and antibacterial activity against Staphylococcus aureus and Escherichia coli," *Anim. Biotechnol.*, 2020, doi: 10.1080/10495398.2020.1842751.
- [2] D. Mu, X. Mu, Z. Xu, Z. Du, and G. Chen, "Removing Bacillus subtilis from fermentation broth using alumina nanoparticles," *Bioresour. Technol.*, vol. 197, pp. 508–511, Dec. 2015, doi: 10.1016/j.biortech.2015.08.109.
- [3] M. A. Al-Kinani, A. J. Haider, and S. Al-Musawi, "Design, Construction and Characterization of Intelligence Polymer Coated Core–Shell Nanocarrier for Curcumin Drug Encapsulation and Delivery in Lung Cancer Therapy Purposes," *J. Inorg. Organomet. Polym. Mater.*, vol. 31, no. 1, pp. 70–79, Jan. 2021, doi: 10.1007/s10904-020-01672-w.
- [4] M. J. Al-Awady, A. A. Balakit, S. Al-Musawi, M. J. Alsultani, A. Kamil, and M. Alabbasi, "Investigation of anti-MRSA and anticancer activity of eco-friendly synthesized silver nanoparticles from palm dates extract," *Nano Biomed. Eng.*, vol. 11, no. 2, pp. 157–169, 2019, doi: 10.5101/nbe.v11i2.p157-169.
- [5] S. Al-Musawi, A. J. Hadi, S. J. Hadi, and N. K. Kadhimi Hindi, "Preparation and characterization of folated chitosan/magnetic nanocarrier for 5-fluorouracil drug delivery and studying its effect in bladder cancer therapy," *J. Glob. Pharma Technol.*, vol. 11, no. 7, pp. 628–637, 2019.
- [6] S. Al-Musawi, M. J. Kadhimi, and N. K. K. Hindi, "Folated-nanocarrier for paclitaxel drug delivery in leukemia cancer therapy," *J. Pharm. Sci. Res.*, vol. 10, no. 4, pp. 749–754, 2018.
- [7] L. Ma'Mani *et al.*, "Curcumin-loaded guanidine functionalized PEGylated I3ad mesoporous silica nanoparticles KIT-6: Practical strategy for the breast cancer therapy," *Eur. J. Med. Chem.*, vol. 83, pp. 646–654, 2014, doi: 10.1016/j.ejmech.2014.06.069.
- [8] M. A. M. Jahromi *et al.*, "Curcumin-loaded chitosan tripolyphosphate nanoparticles as a safe, natural and effective antibiotic inhibits the infection of staphylococcus aureus and pseudomonas aeruginosa in vivo," *Iran. J. Biotechnol.*, vol. 12, no. 3, 2014, doi: 10.15171/ijb.1012.
- [9] S. Albukhaty *et al.*, "Investigation of dextran-coated superparamagnetic nanoparticles for targeted vinblastine controlled release, delivery, apoptosis induction, and gene expression in pancreatic cancer cells," *Molecules*, vol. 25, no. 20, p. 4721, Oct. 2020, doi: 10.3390/molecules25204721.
- [10] S. Al-Musawi *et al.*, "Antibacterial activity of honey/chitosan nanofibers loaded with capsaicin and gold nanoparticles for wound dressing," *Molecules*, vol. 25, no. 20, p. 4770, Oct. 2020, doi: 10.3390/molecules25204770.
- [11] S. Al-Musawi, S. Albukhaty, H. Al-Karagoly, G. M. Sulaiman, M. S. Jabir, and H. Naderi-Manesh, "Dextran-coated superparamagnetic nanoparticles modified with folate for targeted drug delivery of camptothecin," *Adv. Nat. Sci. Nanosci. Nanotechnol.*, vol. 11, no. 4, p. 045009, Dec. 2020, doi: 10.1088/2043-6254/abc75b.
- [12] M. A. Al-Kinani, A. J. Haider, and S. Al-Musawi, "High Uniformity Distribution of Fe@Au Preparation by a Micro-Emulsion Method," *IOP Conf. Ser. Mater. Sci. Eng.*, vol. 987, no. 1, 2020, doi: 10.1088/1757-899X/987/1/012013.
- [13] S. Al-Musawi, S. Albukhaty, H. Al-Karagoly, and F. Almalki, "Design and synthesis of multi-

- functional superparamagnetic core-gold shell coated with chitosan and folate nanoparticles for targeted antitumor therapy,” *Nanomaterials*, vol. 11, no. 1, pp. 1–14, Jan. 2021, doi: 10.3390/nano11010032.
- [14] S. Al-Musawi *et al.*, “Smart nanoformulation based on polymeric magnetic nanoparticles and vincristine drug: A novel therapy for apoptotic gene expression in tumors,” *Life*, vol. 11, no. 1, pp. 1–12, Jan. 2021, doi: 10.3390/life11010071.
- [15] W. J. Al-Kaabi *et al.*, “Development of *Inula graveolens* (L.) plant extract electrospun/polycaprolactone nanofibers: A novel material for biomedical application,” *Appl. Sci.*, vol. 11, no. 2, pp. 1–10, Jan. 2021, doi: 10.3390/app11020828.
- [16] M. A. Al-Kinani, A. J. Haider, and S. Al-Musawi, “Design and Synthesis of Nanoencapsulation with a New Formulation of Fe@Au-CS-CU-FA NPs by Pulsed Laser Ablation in Liquid (PLAL) Method in Breast Cancer Therapy: In Vitro and In Vivo,” *Plasmonics*, pp. 1–11, Jan. 2021, doi: 10.1007/s11468-021-01371-3.
- [17] R. M. Humphries *et al.*, “The continued value of disk diffusion for assessing antimicrobial susceptibility in clinical laboratories: Report from the clinical and laboratory standards institute methods development and standardization working group,” *Journal of Clinical Microbiology*, vol. 56, no. 8. American Society for Microbiology, Aug. 01, 2018, doi: 10.1128/JCM.00437-18.
- [18] A. F. Halbus, T. S. Horozov, and V. N. Paunov, “Colloid particle formulations for antimicrobial applications,” *Advances in Colloid and Interface Science*, vol. 249. Elsevier B.V., pp. 134–148, Nov. 01, 2017, doi: 10.1016/j.cis.2017.05.012.
- [19] E. Hoseinzadeh *et al.*, “A Review on Nano-Antimicrobials: Metal Nanoparticles, Methods and Mechanisms,” *Curr. Drug Metab.*, vol. 18, no. 2, pp. 120–128, Dec. 2016, doi: 10.2174/1389200217666161201111146.
- [20] M. Karthikeyan, S. C. Ahila, and B. Muthu Kumar, “The antibacterial influence of nanotopographic titanium, zirconium, and aluminum nanoparticles against *Staphylococcus aureus* and *porphyromonas gingivalis*: An In vitro study,” *Indian J. Dent. Res.*, vol. 30, no. 1, pp. 37–42, Jan. 2019, doi: 10.4103/ijdr.IJDR-91-16.
- [21] J. Lehtonen *et al.*, “Effects of Chloride Concentration on the Water Disinfection Performance of Silver Containing Nanocellulose-based Composites,” *Sci. Rep.*, vol. 9, no. 1, pp. 1–10, Dec. 2019, doi: 10.1038/s41598-019-56009-6.
- [22] J. Yu *et al.*, “Selective detection for seven kinds of antibiotics with blue emitting carbon dots and Al<sup>3+</sup> ions,” *Spectrochim. Acta - Part A Mol. Biomol. Spectrosc.*, vol. 223, p. 117366, Dec. 2019, doi: 10.1016/j.saa.2019.117366.
- [23] F. Peng *et al.*, “Nanoparticles promote in vivo breast cancer cell intravasation and extravasation by inducing endothelial leakiness,” *Nat. Nanotechnol.*, vol. 14, no. 3, pp. 279–286, Mar. 2019, doi: 10.1038/s41565-018-0356-z.
- [24] M. S. Selim *et al.*, “Design of  $\gamma$ -AlOOH,  $\gamma$ -MnOOH, and  $\alpha$ -Mn<sub>2</sub>O<sub>3</sub> nanorods as advanced antibacterial active agents,” *Dalt. Trans.*, vol. 49, no. 25, pp. 8601–8613, Jul. 2020, doi: 10.1039/d0dt01689f.
- [25] S. Muzammil *et al.*, “Aluminium oxide nanoparticles inhibit EPS production, adhesion and biofilm formation by multidrug resistant *Acinetobacter baumannii*,” *Biofouling*, vol. 36, no. 4, pp. 492–504, Apr. 2020, doi: 10.1080/08927014.2020.1776856.
- [26] A. Khoobi, M. Salavati-Niasari, M. Ghani, S. M. Ghoreishi, and A. Gholami, “Multivariate optimization methods for in-situ growth of LDH/ZIF-8 nanocrystals on anodized aluminium substrate as a nanosorbent for stir bar sorptive extraction in biological and food samples,” *Food Chem.*, vol. 288, pp. 39–46, Aug. 2019, doi: 10.1016/j.foodchem.2019.02.118.
- [27] N. E. Markina and A. V. Markin, “Application of aluminum hydroxide for improvement of label-free SERS detection of some cephalosporin antibiotics in urine,” *Biosensors*, vol. 9, no. 3, Sep. 2019, doi: 10.3390/bios9030091.

- [28] T. Kaur, C. Putatunda, A. Vyas, and G. Kumar, "Zinc oxide nanoparticles inhibit bacterial biofilm formation via altering cell membrane permeability," *Prep. Biochem. Biotechnol.*, vol. 51, no. 4, pp. 309–319, 2021, doi: 10.1080/10826068.2020.1815057.
- [29] R. Chen *et al.*, "Antibacterial activity, cytotoxicity and mechanical behavior of nano-enhanced denture base resin with different kinds of inorganic antibacterial agents," *Dent. Mater. J.*, vol. 36, no. 6, pp. 693–699, 2017, doi: 10.4012/dmj.2016-301.
- [30] J. S. Al-Brahim and A. E. Mohammed, "Antioxidant, cytotoxic and antibacterial potential of biosynthesized nanoparticles using bee honey from two different floral sources in Saudi Arabia," *Saudi J. Biol. Sci.*, vol. 27, no. 1, pp. 363–373, Jan. 2020, doi: 10.1016/j.sjbs.2019.10.006.
- [31] A. Balasubramanyam *et al.*, "Evaluation of genotoxic effects of oral exposure to Aluminum oxide nanomaterials in rat bone marrow," *Mutat. Res. - Genet. Toxicol. Environ. Mutagen.*, vol. 676, no. 1, pp. 41–47, May 2009, doi: 10.1016/j.mrgentox.2009.03.004.
- [32] T. J. Booth and M. A. B. Baker, "Nanotechnology: Building and Observing at the Nanometer Scale," in *Pharmacognosy: Fundamentals, Applications and Strategy*, Elsevier Inc., 2017, pp. 633–643.
- [33] Y. ying Zhang, Q. Liu, C. Yang, S. chuan Wu, and J. hua Cheng, "Magnetic aluminum-based metal organic framework as a novel magnetic adsorbent for the effective removal of minocycline from aqueous solutions," *Environ. Pollut.*, vol. 255, no. Pt 2, Dec. 2019, doi: 10.1016/j.envpol.2019.113226.
- [34] A. E. Mohammed, A. Al-Qahtani, A. Al-Mutairi, B. Al-Shamri, and K. F. Aabed, "Antibacterial and cytotoxic potential of biosynthesized silver nanoparticles by some plant extracts," *Nanomaterials*, vol. 8, no. 6, Jun. 2018, doi: 10.3390/nano8060382.
- [35] E. Radziun *et al.*, "Assessment of the cytotoxicity of aluminium oxide nanoparticles on selected mammalian cells," *Toxicol. Vitro.*, vol. 25, no. 8, pp. 1694–1700, Dec. 2011, doi: 10.1016/j.tiv.2011.07.010.
- [36] D. Lin and B. Xing, "Phytotoxicity of nanoparticles: Inhibition of seed germination and root growth," *Environ. Pollut.*, vol. 150, no. 2, pp. 243–250, Nov. 2007, doi: 10.1016/j.envpol.2007.01.016.
- [37] M. A. Ansari, H. M. Khan, A. A. Khan, S. S. Cameotra, Q. Saquib, and J. Musarrat, "Interaction of Al<sub>2</sub>O<sub>3</sub> nanoparticles with Escherichia coli and their cell envelope biomolecules," *J. Appl. Microbiol.*, vol. 116, no. 4, pp. 772–783, 2014, doi: 10.1111/jam.12423.
- [38] M. A. Ansari *et al.*, "Green synthesis of Al<sub>2</sub>O<sub>3</sub> nanoparticles and their bactericidal potential against clinical isolates of multi-drug resistant Pseudomonas aeruginosa," *World J. Microbiol. Biotechnol.*, vol. 31, no. 1, pp. 153–164, Jan. 2015, doi: 10.1007/s11274-014-1757-2.